Strain Partitioning in West-Central Zagros Fold and Thrust Belt: Implication for Seismic Hazard Analysis

Z. Malekzade[1], M.R. Abbassi[2], O. Bellier[3], and C. Authemayou[3]

1. Payam-e-Nour University, Sari, Iran, email: malekzade04@yahoo.com
2. Seismology Research Center, International Institute of Earthquake Engineering and Seismology (IIEES), I.R. Iran
3. Centre Europe´en de Recherche et d'Enseignement de Ge´osciences de l'Environnement (UMR CNRS 6635), Universite´ Paul Ce´zanne, Aix-en-Provence, Cedex 4, France

ABSTRACT: *This paper provides some documents to reintroduce the active faults and their ability to generate strike-slip earthquakes in west-central Zagros Fold and Thrust Belt (ZFTB). For this purpose, the structural and geomorphic arguments were presented to improve the fault kinematics and segmentation need for calculation of the largest magnitude due to their reactivation within interested area. Slip rates along strike slip faults, which have already been estimated, are used to estimate the probable recurrence interval time of the events. The strike-slip faults extend in N-S direction around 52^{o}E from frontal part of ZFTB to the north and continued along the strike of the Belt, i.e. the Main Recent Fault (MRF), at the rear of the belt. The MRF has been considered as a major dextral strike-slip fault in the context of the tectonic model of the strain partitioning. It was shown that MRF is not unique in the strain partitioning system, but the High Zagros Fault (HZF) in the domain of the High Zagros Belt (HZB) is contributing in the partitioning of strain of the Arabian plate oblique convergence. Therefore, both of HZF and MRF can potentially cause the strike-slip events. Our data shows that the lengths of fault segments along MRF increase toward northwestward. In case of HZF and Kazerun faults, the segments' lengths increase in southeast and northward, respectively. The growth of the length of the segments is in accordance with the increase of the slip-rate. Consequently, it was expected that the seismicity would increase in these directions.*

Keywords: Strain partitionary; Seismic analysis; Thrust belt; West-central Zagros fold

1. Introduction

This study deals with the seismic hazard assessment of the west-central Zagros Fold and Thrust Belt (*ZFTB*), see Figure (1). *ZFTB* is a deforming zone between Arabian plate and a stable part of central Iran (Sanandaj-Sirjan zone) as a consequence of obliquely continental collision. Classically, it was believed that the collision has been started since Tertiary [3, 10, 19]. The suture zone lies on the strike of the Main Zagros Reverse Fault (*MZRF*) that has been turned to become an inactive thrust zone recently [46, 49, 51].

An active fault following the *ZMRF*, firstly introduced by Tchalenko and Braud [47], is the Main Recent Fault (*MRF*). It is partly accommodating the deformation due to oblique collision as right-lateral strike-slip fault. The other important fault that lies in the southwest and is partly parallel with the *MRF* is *HZF*. The *HZF's* activity caused Paleozoic rocks to be uplifted nearly 6*km* and has made one of the highest parts of mountain range in west-central *ZFTB* [11]. The region between the *MZRF* and *HZF*

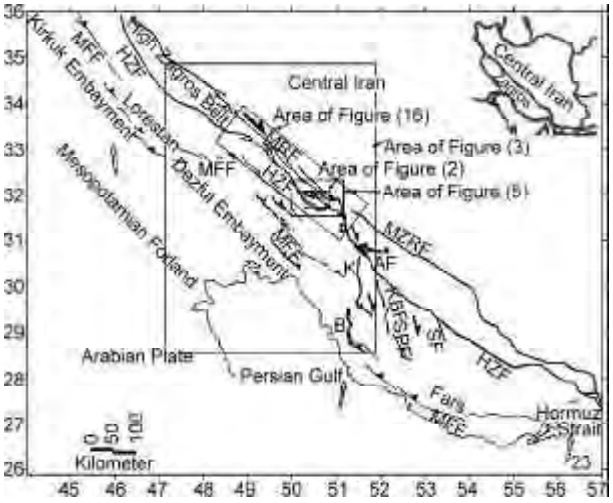

Figure 1. Regional map of Zagros Fold and Thrust Belt (ZFTB) (Modified from [11, 13, 31]) showing the fault pattern and divisions. White arrows show the plate convergence direction [48]. MZRF = Main Zagros Reverse Fault; MRF = Main Recent Fault; HZF = High Zagros Fault; MFF = Mountain Frontal Fault; AF = Ardekan Fault; SPF= Sabzpushan Fault; KBF=Kare-Bass Fault; D, K and B are Kazerun Faults' segments; and SF = Sarvestan Fault.

is called *HZB* (High Zagros Belt), see Figure (1). The *HZB* is characterized by intensively folded and thrust belt. Southwestward, the *HZB* is limited by a less-deformed region namely, Simply Folded Belt. As the name implies, the Simply Folded Belt consists of the large open anticlines that was uplifted and elevated by tectonic activity along the Mountain Frontal Fault (*MFF*), see Figure (1).

The *MRF* terminates around the $51^{o}E$ where *N-S* trending right lateral strike-slip faults of Kazerun Fault transect the *ZFTB*. The deformation flows from *MRF* to a series of *N-S* trending faults as a fan-shaped pattern fault [4]. The Kazerun Fault is considered as being an active and basement fault that reactivates frequently in different modes [8, 11, 17, 18]. It consists of three main strands of Dena, Kazerun and Borazjan from north to south respectively [4, 6, 50].

Reactivation of *HZF*, *MRF* and Kazerun faults has caused the historical and recent quakes to undergo some damage and destructions. To estimate and assess the seismic hazard, it is needed to know the seismic sources and its features. Among the main features are the fault lengths, seismogenic depth and fault slip rate. However, tectonic characterization seems to be important and has a priority for any constraints on these features.

The surface exposure and slip rate of *MRF* and Kazerun faults have comprehensively been studied by Authemayou et al [6], (Quaternary slip-rates along the Kazerun and the Main Recent Faults: evidence for slip partitioning in the Zagros fold and thrust belt, [6]), however, the *HZF's* role in *HZB* domain was not specified to date.

This paper has two main concerns: at first, it aims at clarifying the role of *HZF* in the deformation pattern of west-central Zagros domain. Secondly, using the data already published [6, 11], *CMT* catalog [31], and the evidences obtained by the present work, the paper estimates the maximum magnitude of strike-slip events and their recurrence time within the area covered by *MRF*, *HZF* and Kazerun faults.

2. Geological and Geodynamical Setting

Throughout the Paleozoic, the central Iran was part of the Arabian plate [10, 12, 41, 42, 44]. With opening of the Permo-Teriassic Neo-Tethys Ocean, these regions formed two different sedimentary basins in their own sides. This geological and tectonic evolution of the Zagros (the northeast rim of Arabian plate) has been dominated by a long period of relatively stable platform sedimentation from Cambrian to the Tertiary. It is thought that the *NW*-SE trending linear facies boundaries at this time are the result of the development of normal faults (associated with crustal thinning) parallel to the old continental margin [10, 28], and the majority of which probably dipped towards the northeast [24-25]. At the base of this sedimentary sequence is the thick (1-2*km*) Cambrian Hormuz salt. This layer acts as the major décollement during the Late Tertiary deformation, although other detachment horizons occur in the cover rocks, see Figure (2). The existence of these décollement horizons allows decoupling of the deformation between the basement and cover as well as between different units within the cover sequence which plays an important role in controlling the pattern and distribution of deformation during the basin inversion [38]. The exposure of the Hormuz salt along the major fault zones of *MRF*, *HZF* and Kazerun implies that these faults are deep-seated and may cut the basement fault. The trace of Hormuz salt in *ZFTB* is an indicator for the basement faults such as *MRF*, *HZF* and Kazerun.

Basin inversion under the contractional tectonic regime that generally commenced since the first obduction event in upper Cretaceous [3, 10], controls the recent seismicity within the *ZFTB* [25-26] and southwestward propagation of the deformation [21,

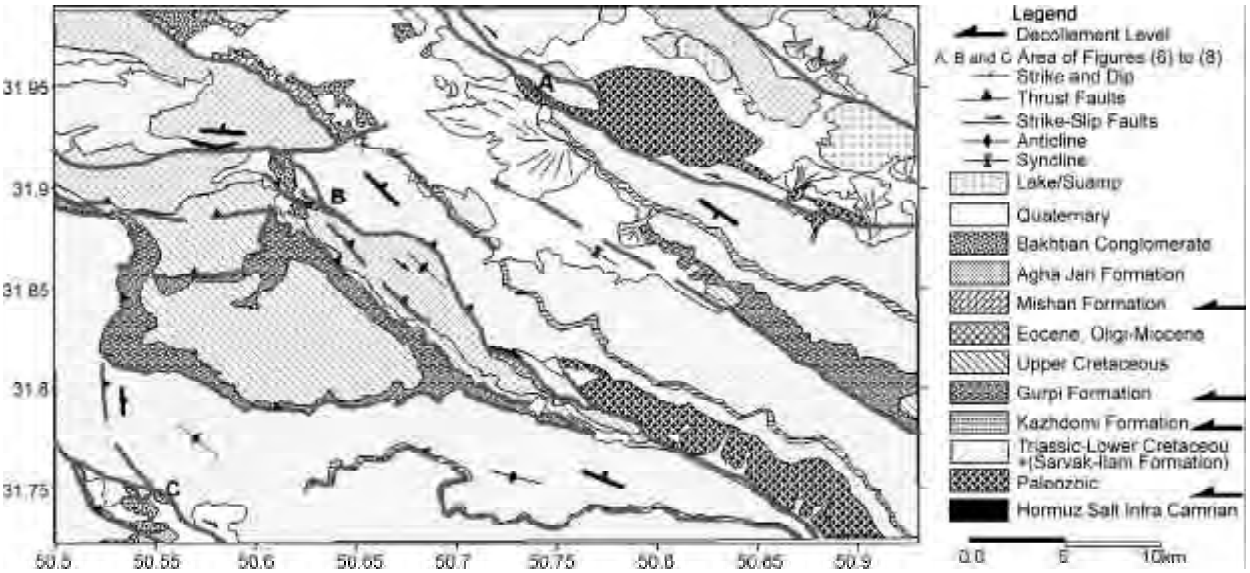

Figure 2. Geological and structural map of west-central High Zagros modified from Geological quadrangle map of Iran, Ardal sheet, sheet 6153, scale 1:100,000 [16]. The decollement horizons are indicated in legend by arrows. Intrusion of salts to the surface and manifestation along strike of the MRF and HZF reveal that the faults are probably originated beneath the basement. From seismic hazard point of view, the faults that cut the basement are more important and demonstrate the regional strain partitioning. A, B and C are located on the area of Figures (6) to (8).

40]. Based on synfolding unconformity of the upper Agha-Jari formation of late Miocene to early Pliocene age, and the abundance and wide distribution of clastic synorogenic sediments of Plio-Quaternary age throughout the Zagros (Bakhtiary Formation), the main regional shortening phase in the fold-and-thrust belt is believed to be started from the late Miocene during the Pliocene [18, 21, 23, 40, 43].

The *HZB* and *SFB* are characterized by the domains exposure of Cretaceous and early Tertiary rocks, respectively. This suggests spatiotemporal activity of *HZF* and *MFF*, as the southern boundary of *HZB* and *ZSFB*. Furthermore, the presence of wedging of the post-Asmari deposits (Miocene Gachsaran evaporites together with the Lower Miocene to Pleistocene Aghajari-Bakhtiari synorogenic molasse) towards the High Zagros [18, 22, 27], suggest the uplift of the High Zagros along the *HZF* since the Early Miocene, which contemporaneous with the relative subsidence of the Zagros Foredeep and southward migration of the Zagros basin and deformation as well as the out-of-sequence activity along *HZF* fault. This, in turn, may infer switching from thin-skinned to thick-skinned tectonic as suggested by Molinaro et al [34] for southeast of Zagros. Transition from thin to thick-skinned tectonic is referred as being the reorganization of continental collision and stress regime change from thrust to strike-slip regime in different parts of the *ZFTB* [5, 29, 35, 37]. It is followed by the onset of *MRF* activity [5] and dominated the strain partitioning tectonic in west Zagros [5, 11, 13, 45].

Roughly *N-S* direction of Arabian plate movement toward central Iran [32] is stable over 19*Ma*. It makes about 45^{o} to the central Iran border. This oblique convergence is not similarly accommodated along strike of the Zagros [45], therefore, over the southeast part of the belt, the orthogonal shortening is dominant. The west of central Zagros, in which a series of *N-S* trending strike-slip fault is present, the system of strain partitioning is dominant. In reality, the strike-slip faults act as the zone by which the deformation mode of partitioning in west change to the orthogonal shortening in southeast.

Based on geomorphic and geological evidences, the degree of partitioning has been discussed [6]. Due to the folding and thrust faulting in this framework, the shortening rate is (among them *HZF*) compared to the dextral displacement along strike of the *MRF*. On the other hand, the *GPS* data [48- 49] shows that the movement along strike of *MRF* is less than the shortening rate deduced by geological documents. The *HZF* was chosen to test the complete partitioning hypothesis. If this is correct, then the *HZF* must have a thrust kinematics, otherwise the hypothesis seems to be improved. It is worth to note that the *HZF* in west-central *HZB* has not been studied yet and is thought to be as a thrust fault according to the geomorphologic data [11]. The outcomes can reveal the role of the *HZF* in

deformational pattern of the *HZB* and its seismotectonic implications.

3. Fault Geometry

Figure (3) demonstrates fault pattern within *HZB* and Central Zagros. The *MRF* and the fan shaped *N-S* strike-slip faults are depicted by Authemayou et al [4]. The *MRF* has two branches: to the northwest they adjoin together near Doroud town and in south-east part, with contribution of Kazerun fault, they make a complex branch point [31]. Transferring the deformation from *MRF* to Kazerun fault is carried out by a system in a similar manner to a left-stepping restraining step-over, see Figure (4).

Concerning the *HZF*, it has been divided to three main parts: *NW* and Central part with more or less straight form and *SE* portion which consists of horse-tail faults. *NW* segment follows a *NW-SE* trend as the *MRF* and general trend of Zagros range. Around 50°*E*, the trend changes to the nearly similar state of the Kazerun fault. This similarity makes a left-stepping arrangement of Kazerun and *HZF*, and the fault pattern south eastern part, seems to be like a horse-tail arrangement faults in a manner of the step-over, see Figure (5).

4. Seismicity within Study Area

Earthquakes, larger than those occur in inner Zagros are taking place along the *MRF* [11]. The fault ruptured almost along its length from Dinevar in the northwest (with the 1957.12.13 event, *Ms*=6.7) to lake Gahar in the southeast (with the 1909.01.23, *Ms*=7.4, and the pre-historic lake Gahar earthquake) in a series of large earthquakes from 1909-1963, see Figure (3).

The historical and instrumental seismicity of the *KF* concentrates along its central part [8, 11, 45],

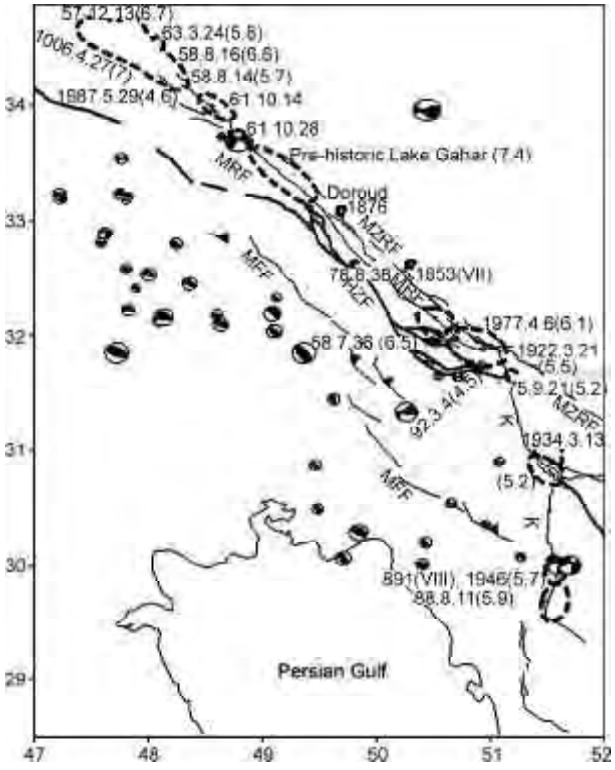

Figure 3. The simplified seismotectonic map of the west-central ZFTB. The focals are earthquakes occurred since 1968 to 2000 and reassessed by Talebian and Jackson [45]. Dated meizoseismals area is drawn by doted closed line. Abbreviations are the same as Figure (1).

Figure 4. Step over made by two left-stepping strike-slip faults of Kazerun fault from south and MRF from NW makes a pop-up structure in their connection point. Elevated young materials in front of structure gave rise to local sliding and gravitational collapses and were reflected as normal faults on the map, see Figure (5) for location.

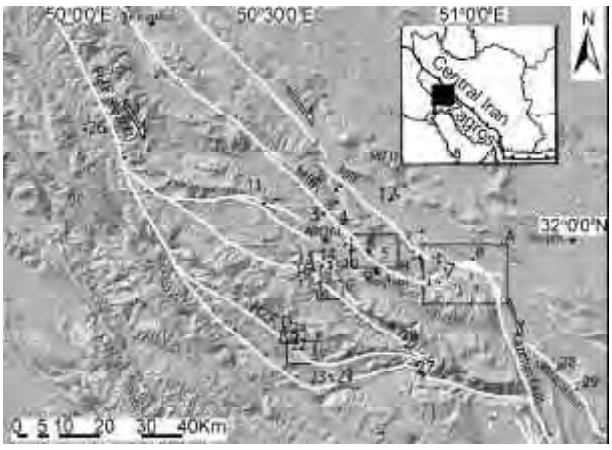

Figure 5. West-central HZB active faults mapped on shaded relief map of SRTM digital elevation model and location of sites in which the fault slip data was measured. Note the higher topography area where the MRF and HZF faults meet the Kazerun fault which seems to be as step-overs. A: Area Figure (4); B: Area Figure (6), C: Area Figures (7), (9), (10) and (11); D: Area Figures (8) and (12); E: Area Figures (13) and (14).

where several historical events of intensity greater than 8, which have repeatedly destroyed the royal city of Bishâpur near Kazerun, have been reported [6 and refrences therein]. Results from a paleoseismological study also suggest that at least two earthquakes of magnitude over 6 occurred during the Holocene [7].

Events, if any, have been reported for *HZF* along the segments west of the Kazerun fault, see Figure (3). The microseismicity and geological evidences reveal that the *HZF* is potentially active [51]. Our seismic reassessment of *HZF* will be associated with the present activity along the fault and segmentation in term of structural documents.

5. Methodology

Combined structural geology and morphology analysis supported by field Spot and Landsat images measurements were used in this study to constrain the quaternary stress regime and fault kinematics. In order to determine the most recent states of stress and highlighting the mode of deformation accommodation within the High Zagros Belt, quantitative inversions of fault slip vectors (striae), measured at individual sites, have been computed using the method initially proposed by Carey [15] based on theoretical approaches presented by Bott [14]. Fault/striae have been measured in 29 stations indicated in Figure (5). They affected Paleozoic to Plio-Quaternary rocks within the *HZB*. In all sites, the stress tensor is regarded as the recent stress regimes.

Geomorphic features containing the drainage and ridge offsets helped to confirm the present-day kinematics obtained by inversion and to estimate the horizontal slip rate of both strike-slip and thrust faults. Using data presented by cosmic ray exposure dating analysis [6], the geometry of faults including fault length and total offset of fan deposits by fault activity, it could be possible to compute the time recurrence of earthquake and its moment magnitude.

5.1. Inversion Results, Structural and Geomorphic Features

To determine the dominant kinematics, three points across the High Zagros were selected, as shown in Figure (2), where the surface exposure of *MRF* and *HZF* can be seen. The fault slip inversion results measured on the faults is presented in this study. At the first step, point A in Figure (2), our data show a strike-slip regime for *MRF*, as shown in Figure (6), in agreement with previous studies [5-6]. By opposition, the *HZF* (point *B* on the *HZF*) does not

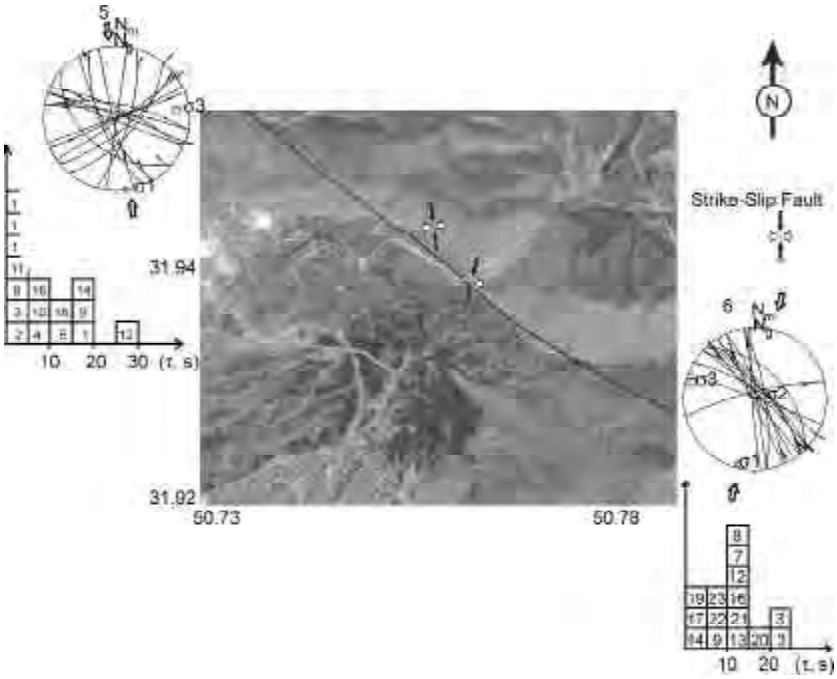

Figure 6. Lower-hemisphere stereoplots showing strike-slip faulting near the Naghan City (stations 5 and 6 in Figure (5)) together with results determined by the inversion method of Carey [15]. Individual fault planes and measured slip vectors at each site are plotted, arrows on fault planes point in directions of horizontal azimuth of the slip vectors. Stress axes obtained by inversions are shown by diamond (σ_1), triangle (σ_2) and square (σ_3). Histogram shows the distribution of deviation angles between the measured 's' and the predicted 'τ' slip vector on each fault plane. Large arrows outside stereoplots give the azimuth of the maximum horizontal stress (σ_1).They indicate a strike-slip stress regime with σ_1 axis roughly N-S. Stream offset confirms the right-lateral displacing along the fault.

merely show a thrust regime; rather it demonstrates a mix mode of tectonic regime. In the higher elevation regions, strike-slip faults are dominant and within lower level, it is accompanied by thrust faults, see Figure (7). The σ_1 direction on the strike-slip faults shows a nearly *N-S* trending (station 15 in Figure (7)) and on the thrust faults they align toward northeastward characterizing a strain partitioning system. Our observations on the field show that the young sediment (Bakhtiary conglomerate) are cut at least by two events. The younger events have the lower rake on the fault planes. Based on the observations, it is suggested that each of major branch of *HZF* follows this rule, i.e. the association of a higher dip angle fault with a component of strike-slip parallel to the *ZFTB* and a set of low angle thrust faults with the same strike.

Figure (8) and point *C* in Figure (2) show the

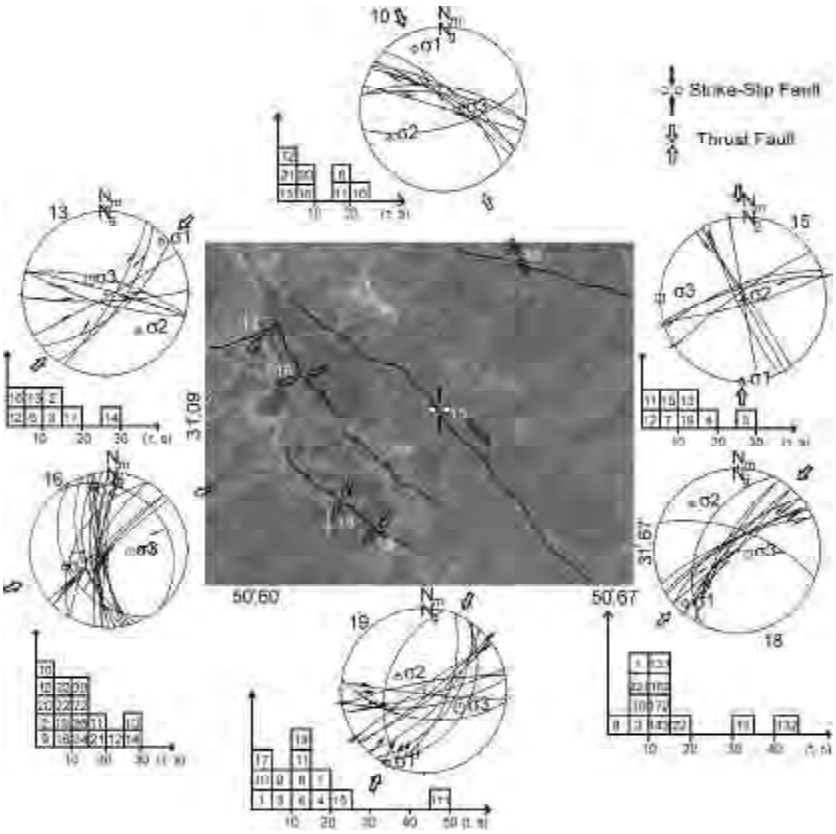

Figure 7. Lower-hemisphere stereoplots showing both strike-slip and thrust faulting from along strike of the HZF together with results determined by the inversion method fault-slip analysis. Strike-slip activity with thrust faulting, both of which affect the young sediments, imply the strain partitioning at local scale. Data description is the same as Figure (6), see Figure (5) for location.

Figure 8. Lower-hemisphere stereoplots showing strike-slip faulting along HZF, see Figure (5) for location. The fault affected the Bakhtiary conglomerate implying the recent strike-slip stress regime. The arrow is the location of the cross section shown in Figure (9).

other segment of *HZF* which indicates the thrust and strike-slip faults in accommodation of deformation. Some low angle thrust faults are accompanied with the higher dip angle strike-slip fault, see Figure (9). It suggests three phases of tectonic activities: first of all, a thin skinned-tectonic caused the Cretaceous rocks to be thrust over Mishan formation through detachment horizon. It is followed by an out-of-sequence phase which caused the accumulation of Aghajari and Bakhtiary conglomerates and finally or contemporaneously thick-skinned tectonic with a strike-slip kinematics, see Figure (8).

It is worth mentioning that structural and geomorphic evidences have comprehensively been presented [6] to show the different aspects of fault activity of the *MRF* and the Kazerun faults. Accordingly, Figure (6), is a station along strike of our transverse section over the *HZB*. Figure (2), demonstrates the dextrally offset of stream by *MRF* activity in agreement with the fault inversion results.

Figure (10) indicates the fan and stream offset along strike of *HZF*. As was defined, the mean offset seems to be 220*m*. These results assert the data presented in Figure (7) at station 15. Furthermore,

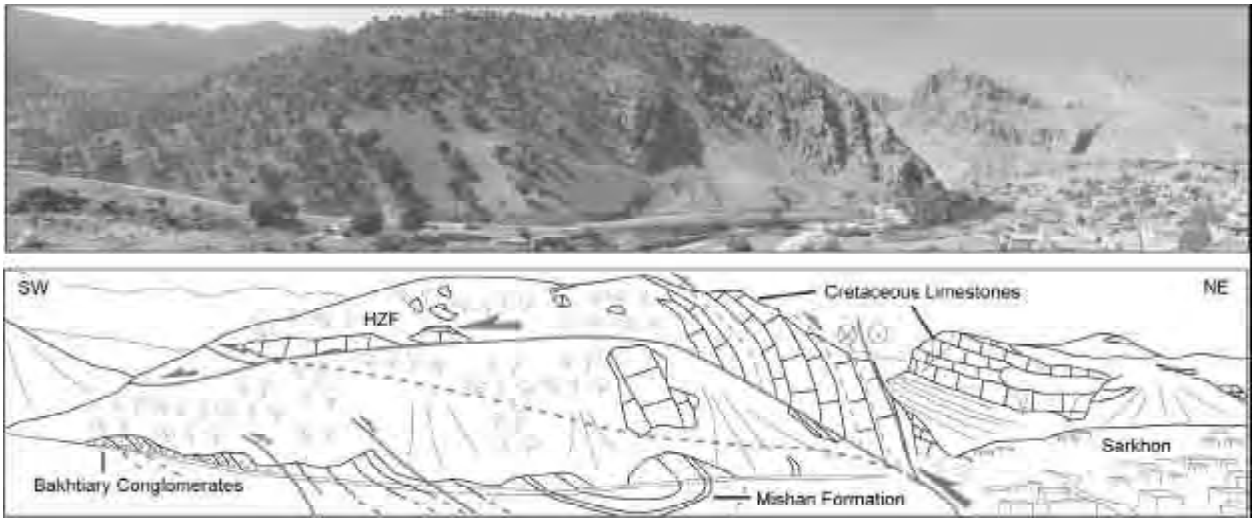

Figure 9. A photo and sketch at point C in Figure (2) on HZF, taken nearby Sarkhon village, as can also be seen in Figure (8), depicting the strike-slip fault together with thrust faults. See text for more explanations.

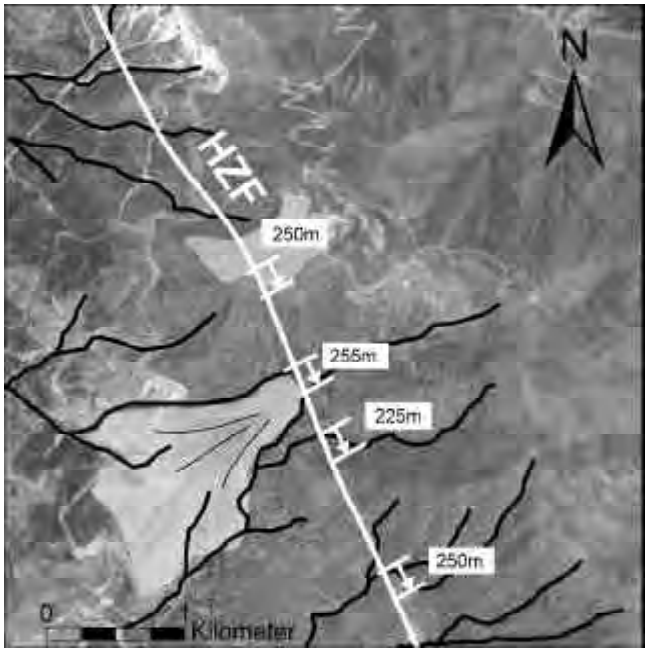

Figure 10. Geomorphic evidences showing the right lateral motion along strike of the HZF for location, see Figure (5). The offsets of the fan, streams and ridge are evident.

the field observations at that station, showed a major flower structure associated with strike-slip faulting that affected both Asmari formation and recent deposits, see Figure (11).

Moreover, Figure (12) presents a 3*D*-view over *HZF* where it is partly covered by the area shown in Figure (7). As can be seen, the fan, ridge and stream dextrally were displaced along the central strike-slip fault. Towards downhill, faults with thrust kinematics affecting the Bakhtiary Conglomerate are dominant. The inversion result also shows the two generations fault/striae that the faults with lower rake are younger implying the change of thrust stress regime to the transpressional tectonic regime.

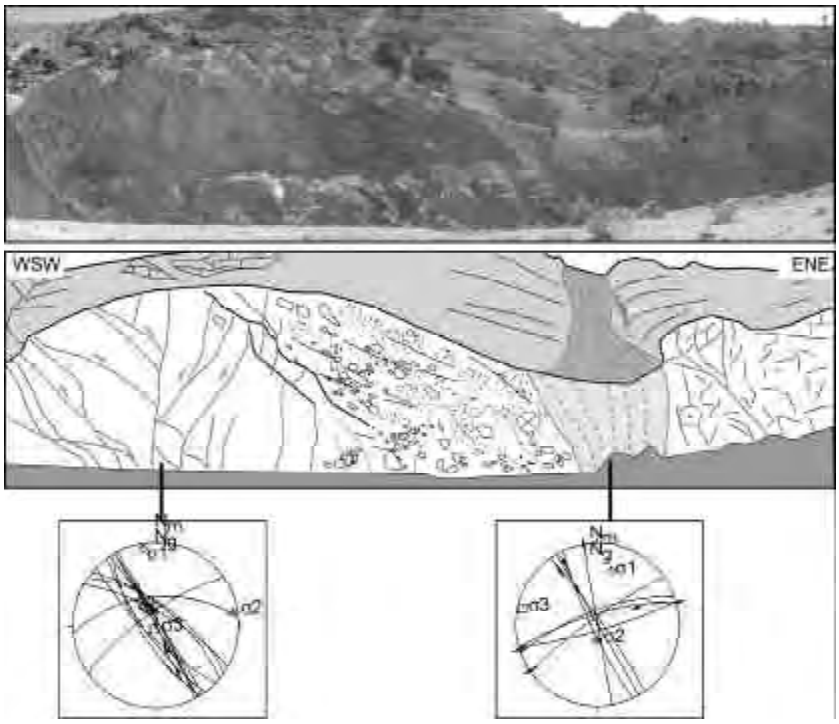

Figure 11. Section across the segment 4 of HZF. Photo shows a flower structure developed by a strike-slip stress regime deduced by inversion method. Fault affected the debris as young sediment material. Lower-hemisphere stereoplots show both the strike-slip and thrust faulting indicating a flower structure, see Figure (5) for location.

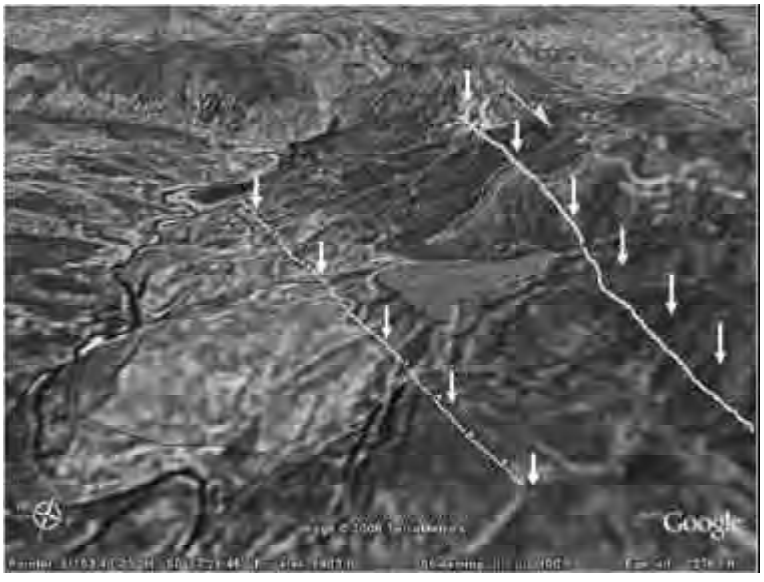

Figure 12. Side view of Google image of segment 12 of HZF gives better constraints on the fault assemblage associated with this segment implying local partitioning. Ridge and stream are dextrally offset by the fault in upstream and the downward the thrust faults are dominated and affected the fan deposits. The Karun river flows west part in a deep valley made by the HZF activity, see Figure (5) for location.

As shown in Figure (13), the southern segment of *HZF* cuts both the bed rock and Bakhtiary Conglomerate. Likewise other segment, it contains fault planes with transpressional strike-slip kinematics. It is the higher angle in central part affecting the Cretaceous limestone and several low angles thrust faults causing the Cretaceous rocks to be thrust on Bakhtiary Conglomerate through a basal décollement of Mishan Formation. A side looking picture on southern branch of *HZF*, shown in Figure (13), gives a 3D-view representing more detailed structural and geomorphic information of the transpressional stress regime over southern *HZF*. According to the displaced fan and stream, shown in Figure (14), it is possible to estimate the recent overall horizontal displacement. The fan also shows the beheaded form suggesting the transpressional stress regime acting on the fault. More evidences, containing the fault kinematics data and geomorphic features, have been presented by Malekzade [31] to confirm the role of the transpressional tectonic regime in crustal deformation.

5.2. Fault Segmentation and Slip Rate

Figure (15) shows the fault pattern in central Zagros. Kazerun fault, as an *N-S* trending fault, has an important role in accommodating the strain from *MRF* and *HZF* to the Fars frontal faults. Authemayou et al [5] segmented the Kazerun fault to the 3 strands where each one terminates to the thrust faults. Recent strike-slip kinematics for Kazerun fault has been justified by other studies [8, 36, 39]. Eastward, the Kazerun fault is associated by other faults with the

Figure 13. Side view of Google image of HZF, see Figure (5) for location. Stream offset dextrally by the fault in higher level and the downward direction of the thrust faults caused the active folding and affects the fan deposits in which fault scarp is clear. The figure also implies a local partitioning of deformation.

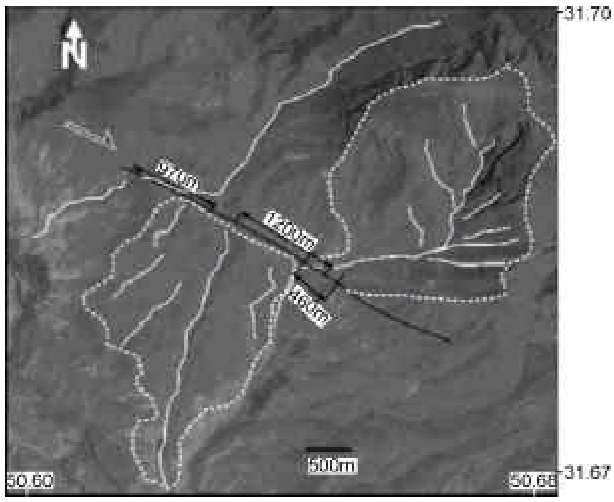

Figure 14. Alluvial fan on Landsat image displaced by HZF, see Figure (5) for location. Considering the age of 140ka, given by Authemayou et al [6] and at least 460m offset of fan, the slip rate and earthquake recurrence time were calculated, see Table (1). Notice the beheaded fan implying the presence of the compressional component along HZF.

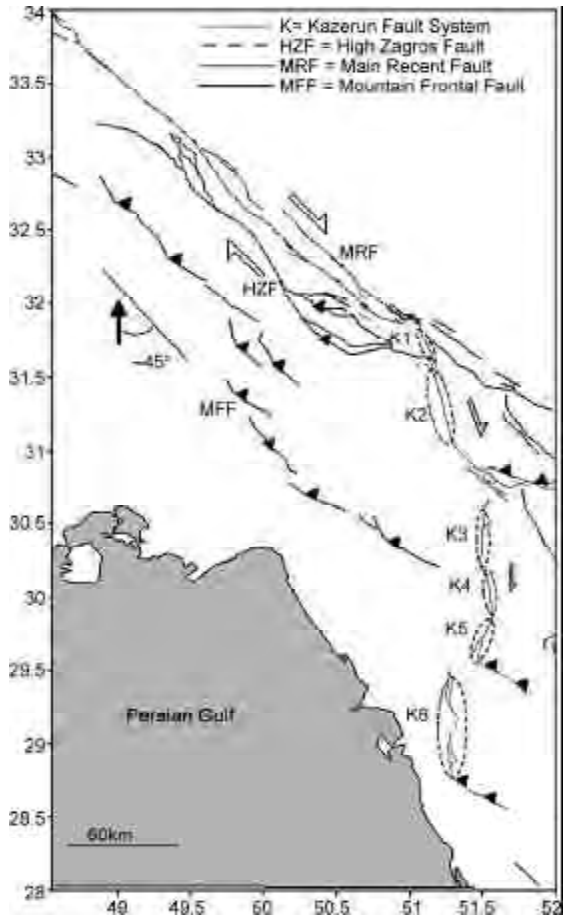

Figure 15. Fault segmentation of Kazerun Fault. The location is shown on Figure (1). Black-filled arrows show the convergence direction and the angle that it makes with the plate boundaries is shown. Open arrows demonstrate the strike-slip kinematics with southward decreasing in slip rate. Filled triangles show the thrust fault, see Figure (5) for location.

same kinematics and strike described as fan-shaped strike-slip faults [e.g. 5].

Based on the surface exposure of fault traces, the segmentation was carried out, see Figures (15) and (16). Each segment was identified using surface fault geometry, meizoseismal area of earthquakes and slip rate [e.g. 9]. The surface geometry contained major flexures or steps that could be a barrier. Barriers, indeed, controls the rupture propagation [1]. The maximum step length, which the earthquake can jump across, is estimated to be 5*km* [20]. Our segmentation shows the increasing length of *MRF's* segments and its slip rate northwestward. Conversely, *HZF's* segments are decreased southeastward, see Figure (16). Apart from some exceptions, Kazerun's segments and its strike-slip activities increase northward.

The slip rates for *MRF* and Kazerun faults have been estimated from lateral offsets of streams, fans and terraces, in situ cosmogenic 36*Cl* exposure

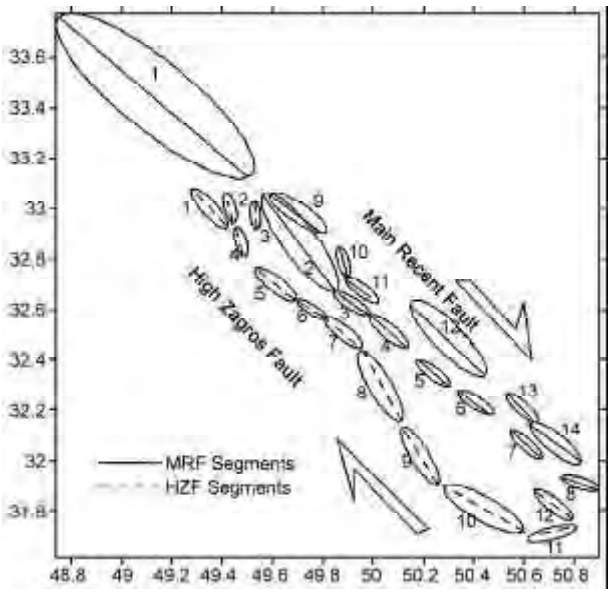

Figure 16. Fault segmentation along HZF and MRF using spot and Landsat satellite images and field work observations. The segments are separated by steps, see Figure (5) for location. The length of the segments is given in Table (1).

Table 1. Calculation of recurrence time of strike-slip earthquakes of given magnitude was computed by faults segments length and slip rates. Columns are segment numbers that were defined in Figure (3), length of fault segment, moment magnitude calculated by relationship (1) seismic moment calculated by (3) displacement of fault per event, displacement of fan deposit due to earthquake, exposure time of sample given on fan surface, slip rate yielded by division of fan offset on exposure time, and recurrence time yielded by division of D by slip rate.

Fault	Segment	Length (km)	Magnitude	M_0 (Dyn/cm)*e26	D (m) (Rupture Per Event)	Fan Offset (m)	Exposure Time (ka)	Slip Rate (mm/year)	Recurrence Interval (Year)
MRF	1	100	7.8-7.0	5.5-0.5	12.2 - 1.0	200-260	19-65	3.1-13.7	73-3935
MRF	2	49	7.4-6.7	14 - 1	6.2 - 0.6	730-780	121-169	3.8-5.5	109-1632
MRF	3	14	6.6 - 6.1	1.2 – 0.2	1.9 – 0.2	730-780	121-169	3.8-5.5	36-500
MRF	4	18	6.8 – 6.2	1.9 – 0.3	2.4 – 0.3	730-780	121-169	3.8-5.5	54-631
MRF	5	16	6.7 – 6.2	1.5 – 0.2	2.2 – 0.3	730-780	121-169	3.8-5.5	54-579
MRF	6	14	6.6 – 6.1	1.2 – 0.2	1.9 – 0.2	730-780	121-169	3.8-5.5	36-500
MRF	7	17	6.7 – 6.2	1.7 – 0.2	2.3 – 0.3	730-780	121-169	3.8-5.5	54-605
MRF	8	14	6.6 – 6.1	1.2 – 0.2	1.9 – 0.2	730-780	121-169	3.8-5.5	36 -500
MRF	9	23	6.9 – 6.3	3.2 – 0.4	3.1 – 0.4	40-166	36-69	1.1-2.1	190-2818
MRF	10	12	6.5 – 6.0	0.9 – 0.1	1.7 – 0.3	40-166	36-69	1.1-2.1	143-1545
MRF	11	12	6.5 – 6.0	0.9 – 0.1	1.7 – 0.3	40-166	36-69	1.1-2.1	143-1545
MRF	12	41	7.2 – 6.6	10 - 1	5.3 – 0.6	40-166	36-69	1.1-2.1	286-4818
MRF	13	14	6.6 – 6.1	1.2 – 0.2	1.9 – 0.2	40-166	36-69	1.1-2.1	95-1727
MRF	14	25	7.0 – 6.4	3.7 – 0.5	3.3 – 0.4	40-166	36-69	1.1-2.1	190-3000
HZF	1	21	7.2-6.6	9 - 1	5.1-0.6	460-970	121-169	2.7 – 8.0	75-1889
HZF	2	9	6.4 – 5.9	0.5 – 0.1	1.3 – 0.2	460-970	121-169	2.7 – 8.0	25-481
HZF	3	11	6.5 – 6.0	0.8 – 0.1	1.5 – 0.2	460-970	121-169	2.7 – 8.0	25-555
HZF	4	11	6.5 – 6.0	0.8 – 0.1	1.5 – 0.2	460-970	121-169	2.7 – 8.0	25-555
HZF	5	20	6.8 – 6.3	2.4 – 0.3	2.7 – 0.4	460-970	121-169	2.7 – 8.0	50-1000
HZF	6	11	6.5 – 6.0	0.8 – 0.1	1.5 – 0.2	460-970	121-169	2.7 – 8.0	25-555
HZF	7	16	6.7 – 6.2	1.6 – 0.2	2.2 – 0.3	460-970	121-169	2.7 – 8.0	38-814
HZF	8	34	7.2 – 6.5	6.8 – 0.8	4.4 – 0.5	460-970	121-169	2.7 – 8.0	63-1630
HZF	9	27	7.0 – 6.4	4.3 – 0.5	3.4 – 0.4	460-970	121-169	2.7 – 8.0	50-1259
HZF	10	36	7.1 – 6.5	7.6– 0.9	4.6 – 0.5	460-970	121-169	2.7 – 8.0	63-1704
HZF	11	14	6.6– 6.1	1.2 – 0.2	1.9 – 0.3	460-970	121-169	2.7 – 8.0	38-704
HZF	12	18	6.8-6.2	2.0 - 0.3	2.4 – 0.3	225-255	121-169	1.3 – 2.1	143-1846
Kazerun	1	45	7.3-6.7	12 – 1.2	5.8-0.6	530-570	121-169	3.1-4.7	128-1871
Kazerun	2	82	7.6-6.9	37 - 3	10.1-0.9	530-570	121-169	3.1-4.7	191-3258
Kazerun	3	48	7.3-6.7	13 – 1.3	6.1-0.6	50-110	22-59	3.1-4.7	128-1968
Kazerun	4	34	7.1-6.5	7 - 0.8	4.4-0.5	50-110	22-59	3.1-4.7	106-1419
Kazerun	5	28	7.0-6.4	4.5 - 0.6	3.7-0.4	50-110	22-59	3.1-4.7	85-1193
Kazerun	6	75	-	-	-	-	-	0.0	No Strike-Slip Event

ages of cobbles sampled on the surface of these geomorphic features, as well as a *U-Th* dating of calcretes cementing the cobbles [6]. For *HZF*, the slip rate was calculated, as can be seen in Table (1), using stream offset, shown in Figures (10) and (14), and dating resulted on fan deposits offset by the *MRF* [6].

In order to calculate the recurrence time of strike-slip earthquakes, an inverse method was used. At first, using the fault segment length (L) and the Wells and Copersmith [51] relationship, the moment magnitude was calculated:

$$Mw = 5.02\ (\pm 0.16) + 1.19\ (\pm 0.1)\ log\ L \qquad (1)$$

Then, using the Mw, the M_0 was computed by Hanks and Kanamori [19] relationship:

$$Mw = (log\ (M_0) - 16.1)\ /1.5 \qquad (2)$$

The moment magnitude scaling law method presented by Hanks and Kanamori [19] was used to compute the displacement per event:

$$M0 = \mu .D .L .h \qquad (3)$$

Where μ is the rigidity or shear modulus (usually taken to about $3*10^{11} dyne/cm^2$), L is the fault length, h is the thickness of seismogenic layer and D is the average displacement over the slip surface [2]. Finally having D and slip rates, the time recurrence was calculated, see Table (1).

6. Discussion

The stress regime change along Zagros has been discussed by some authors in different places along *ZFTB* [e.g., 29, 35, 37] and the others considered the *HZF* as a thrust fault in their model [e.g. 6]. As discussed, the west-central *HZB* differ in tectonic regime with respect to the other parts [e.g. 45]. In addition, the change of fault activity from thin to thick- skinned within and across the *ZFTB* [33-34] without change in fault kinematics has already been envisaged. This study has deciphered the change both in fault kinematics, i.e. change of reverse tectonic regime to the transpresstion one, and fault activity from thin to thick-skinned (as out-of-sequence reactivation) along *HZF* as a major pre-existing structural weakness, see Figure (13). Thick young sediments comprising Agha-Jary and Bakhtiary Formations along *HZF* might imply its out-of-sequence activity. Therefore, the oblique convergence is neither accommodated via a homogenous simple transpressional zone nor a strain partitioning in simple transpression. It seems the major basement faults of *HZF* act as weakness *HZB* boundaries that are locally accommodating the oblique convergence. Each of these faults has simple shear zone along its own length to take up the strike-parallel component of oblique convergence and a pure shear zone in its vicinity to absorb the strike-normal component. Hence, a strike-slip fault was observed (in simple shear zone) accompanying the thrust faults (in pure shear zone). Strike-slip component of *HZF* kinematics could be accounted for the decreasing slip rate along *MRF*. Considering the stability of Arabian plate convergence since 19*Ma* [e.g. 32] as well as the commencement of the stress change in west *ZFTB* since 3-5*Ma* [e.g. 5, 45], it is suggested that the change of the tectonic regime and onset of the partitioning is not a consequence of the plate convergence direction [e.g., 5, 31].

The partitioning is also occurring with depth [e.g. 51] so that in the relatively strong, brittle upper crust, deformation is localized on pre-existing faults (strike-slip). Deformation may occur more easily, and shortening is accommodated by reverse dip-slip faulting perpendicular to the shortening direction. The depth limiting these two different zones might occur within a region of rheological change (such as the base of the seismogenic crust), as envisaged by Lettis and Hanson [30]. The best fitting for the depth of seimogenic layer is considered 15*km* [45, 51].

Accordingly, a majority of events within *HZB* are governed by the strike-slip faults, although the events with thrust kinematics must not be ignored. As stated by Authemayou et al [6], there is a compressional component of slip on each fault system, e.g. site 1 on *MRF* and segment 10 of *HZF* indicated in Figure (13), that may make a thrust event during the fault activities. For example, the biggest event in microearthquake surveying developed by Yaminifard et al [51] and the Ardal earthquake, of 1977.4.6 (Ms = 6.1), shown in Figure (3) *MRF* [11] with a thrust centroid moment tensor.

7. Conclusion

The fact that the strike-slip faults, as a consequent of stress change, are dominant in *HZB* has been discussed and formed the basis for re-assessment of strike-slip earthquakes hazard in West High Zagros. It made the seismic hazard assessment easy in the way that: 1) segmentation was estimated by the accumulated surface rupture along one fault, 2) by considering the previously obtained exposure time [6], the slip rate was calculated, and 3) slip per

event could be estimated, see Table (1). Consequently, the slip per event, length of the fault segment and the depth of seismogenic layer were served to calculate the magnitude of each event. Our analysis shows the northward seismicity along the Kazerun fault. In the case of *MRF*, the segmentation, relatively, shows an increase of lengthening north- westward. This may be related to the growth of the slip rate. *HZF* fault segmentation depicts the longer segments in southeast part. Therefore, the seismicity is expected to be increased southeastward.

Acknowledgments

This work was supported by a cooperative research program between International Institute of Earthquake Engineering and Seismology (*IIEES*, Iran) and the *CNRS* (France), supervised by M.G. Ashtiany and D. Hatzfeld. We thank *IIEES* for fieldwork assistance of M. Mokhtari and M. Zare for support and administrative assistance. Funding was also provided by *IIEES*. We thank I. Shabanian, K. Hessami, M. Zare, F. Yaminifar, A. Saidi, M. Qarashi and M. Massibaigi for their fruitful discussions and constructive comments during the course of this project. We are also grateful to Y. Izadkhah for improving the English of this manuscript.

References

1. Aki, K. (1984). "Asperities, Barriers, and Characteristic Earthquakes", *J. Geophys. Res.*, **89**, 5867-5872.

2. Aki, K. (1966). "Generation and Propagation of G-Waves from the Niigata Earthquake of June 19, 1964. 2. Estimation of Earthquake Movement, Released Energy, and Stress-Strain Drop from G-Wave Spectrum", Bull, Earthquake Res. Inst. (Tokyo Univ.), **44**, 23-88.

3. Alavi, M. (1994). "Tectonics of the Zagros Orogenic Belt of Iran: New Data and Interpretations", *Tectonophysics*, **229**, 211-238.

4. Authemayou, C., Bellier, O., Chardon, D., Malekzadeh, Z., and Abbassi, M.R. (2005). "Role of the Kazerun Fault System in Active Deformation of the Zagros Fold-and-Thrust Belt (Iran)", C. Acad. Sci., Geoscience, **337**, 539-545.

5. Authemayou, C., Chardon, D., Bellier, O., Malekzade, Z., Shabanian, I., and Abbassi, M.R. (2006). "Late Cenozoic Partitioning of Oblique Plate Convergence in the Zagros Fault-and-Thrust Belt (Iran)", *Tectonics*, **25**(TC3002), doi:10.1029/2005TC001860.

6. Authemayou, C., et al (2007). "Quaternary Slip-Rates Along the Kazerun and the Main Recent Faults: Evidence for Slip Partitioning in the Zagros Fold and Thrust Belt", *Submitted to J. of Geophys. Res.*

7. Bachmanov, D.M., Trifonov, V.G., Hessami, K.T. Kozhurin, A.I., Ivanova, T.P., Rogozhin, E.A., Hademi, M.C., and Jamali, F.H. (2004). "Active Faults in the Zagros and Central Iran", *Tectonophysics*, **380**, 221-241.

8. Baker, C., Jackson, J., and Priestley, K. (1993). "Earthquakes on the Kazerun line in the Zagros Mountains of Iran: Strike-Slip Faulting within a Fold-and-Thrust Belt", *Geophys. J. Int.*, **115**, 41-61.

9. Bellier, O., Sebrier, M. Pramumijoyo, S. Beaudouin, Th., Harjono, H., Bahar, I., and Forni, O. (1997). "Paleoseismicity and Seismic Hazard Along the Great Sumatran Fault (Indonesia)", *J. Geodynamics*, **24**(1-4), 169-183.

10. Berberian, M. and King, G.C.P. (1981). "Towards a Paleogeography and Tectonic Evolution of Iran", *Can. J. Earth Sci.*, **18**, 210-285.

11. Berberian, M. (1995). "Master Blind Thrust Faults Hidden under the Zagros Folds Active Basement Tectonics and Surface Morphotectonic", *Tectonophysics*, **241**, 193-224.

12. Beydoun, Z.R., Hughes Clarke, M.W., and Stoneley, R. (1992). "Petroleum in the Zagros Basin: A Late Tertiary Foreland Basin Overprinted Onto the Outer Edge of a Vast Hydrocarbon-Rich Palaeozoic-Mesozoic Passive Margin Shelf", American Association of Petroleum Geologists, Memoir, **55**, 309-339.

13. Blanc, E.J.-P., Allen, M.B., Inger, S., and Hassani, H. (2003). "Structural Styles in the Zagros Simple Folded Zone, Iran", *J. Geol. Soc. London*, **160**, 401-412.

14. Bott, M.H.P. (1959). "The Mechanism of Oblique Slip Faulting", *Geol. Mag.*, **96**, 109-117.

15. Carey, E. (1979). "Recherche Des Directions Principales de Contraintes Associe´es au jeu D'une Population de Failles", *Rev. Geol. Dyn. Geogr. Phys.*, **21**, 57-66.

16. Ehsanbakhsh Kermani, M.H. (1996). "Geological Quadrangle Map of Iran, Ardal Sheet, Sheet 6153, Scale 1:100,000", Geol. Surv. of Iran.

17. Falcon, N.L. (1969). "Problems of the Relationship between Surface Structure and Deep Displacements Illustrated by the Zagros Range", In: P.E. Kent, G.E. Satterthwaite and A.M. Spencer (Editors), Time and Place Orogeny. Geol. Soc. London, Spec. Publ., **3**, 9-22.

18. Falcon, N.L. (1974). "Southern Iran: Zagros Mountains", In: A.M. Spencer (Editor), Mesozoic-Cenozoic Orogenic Belts, Data for Orogenic Studies, *Geol. Soc. London, Spec. Publ.*, **4**, 199-211.

19. Hanks, T.C. and Kanamori, H. (1979). "A Moment Magnitude Scale", *J. Geophys. Res.*, **84**, 2348-2350.

20. Harris, R.A. and Day, S.M. (1993). "Dynamics of Fault Interaction: Parallel Strike-Slip Faults", *J. Geophys. Res.*, **98**, 4461-4472.

21. Hessami, K., Koyi, H.A., and Talbot, C.J. (2001a). "The Significance of Strike-Slip Faulting in the Basement of the Zagros Fold and Thrust Belt", *J. Petrol. Geol.*, **24**, 5-28.

22. Huber, H. (1977). "Geological Map of Iran", 1:1,000,000 with Explanatory Note. Nat. Iran. Oil Co. Explor. Prod. Affairs, Tehran.

23. Haynes, S.J. and McQuillan, H. (1974). "Evolution of the Zagros Suture Zone, Southern Iran", Geol. Soc. Am. Bull., **85**, 739-744.

24. Jackson, J.A. (1980). "Reactivation of Basement Faults and Crustal Shortening in Orogenic Belts", Nature, **283**, 343-346.

25. Jackson, J.A. and Fitch, T. (1981). "Basement Faulting and the Focal Depths of the Larger Earthquakes in the Zagros Mountains (Iran)", *Geophys. J. R. Astron. Soc.*, **64**, 561-586.

26. Jackson, J.A. and McKenzie, D.P. (1988). "The Relationship between Plate Motion and Seismic Moment Tensors, and the Rates of Active Deformation in the Mediterranean and Middle East", *Geophys. J. R. Astron. Soc.*, **93**, 45-73.

27. James, G.S. and Wynd, J.G. (1965). "Stratigraphic Nomenclature of Iranian Oil Consortium Agreement area", *Am. Assoc. Pet. Geol.*, **49**(12), 2182-2245.

28. Koop, W.J. and Stoneley, R. (1982). "Subsidence History of the Middle East Zagros Basin, Permian to Recent", Philosophical Transactions of the Royal Society of London, Series A, **305**, 149-168.

29. Lacombe, O., Mouthereau, F., Kargar, Sh., Meyer, B. (2006). "Late Cenozoic and Modern Stress Fields in the Western Fars (Iran): Implications for the Tectonic and Kinematic Evolution of Central Zagros", *Tectonics*, **25**(TC1003), doi:10.1029/ 2005TC001831.

30. Lettis, W.R. and Hanson, K.L. (1991). "Crustal Strain Partitioning Implications for Seismic Hazard Assessment in Western California", *Geology*, **19**, 559-562.

31. Malekzade, Z. (2007). "Accommodation of Deformation from Main Recent Fault to the Kazerun Fault", Ph.D Thesis, p. 198, International Institute of Earthquake Engineering and Seismology (IIEES), Iran.

32. McQuarrie, N., Stock, J.M., Verdel, C., and Wernicke, B.P. (2003). "Cenozoic Evolution of Neotethys and Implications for the Causes of Plate Motions", G*eophys. Res. Lett.*, **30**(20), 2036, doi:10.1029/ 2003GL017992.

33. Molinaro, M., Letrumy, P., Guezou, J.-C. , Frizon de Lamotte, D., and Eshraghi, S.A. (2005a). "The Structure and Kinematics of the South-Eastern Zagros Foldthrust Belt, Iran: From Thin-Skinned to Thick-Skinned Tectonics", *Tectonics*, **24**(TC3007), doi:10.1029/2004TC001633.

34. Molinaro, M., Zeyen, H., and Laurencin, X. (2005b). "Lithospheric Structure Underneath the South-Eastern Zagros Mountains, Iran: Recent Slab Break-off?", Terra Nova, **17**, 1-6.

35. Navabpour, P., Angelier, J., Barrier, E. (2007).

"Cenozoic Post-Collisional Brittle Tectonic History and Stress Reorientation in the High Zagros Belt (Iran, Fars Province)", *Tectonophysics*, **432**, 101-131.

36. Pattinson, R. and Takin, M. (1971). "Geological Significance of the Dezful Embayement Boundaries", Rep. 1166, Natl. Iran. Oil Co., Tehran.

37. Regard, V., Bellier, O., Thomas, J.-C., Abbassi, M.R. Mercier, J.L., Shabanian, E., Feghhi, K., and Soleymani, S. (2004). "The Accommodation of Arabia-Eurasia Convergence in the Zagros-Makran Transfer Zone, SE Iran: A Transition between Collision and Subduction Through a Young Deforming System", *Tectonics*, **23**(TC4007), doi:10.1029/2003TC001599.

38. Sepehr, M. and Cosgrove, J.W. (2004). "Structural Framework of the Zagros Fold-and-Thrust Belt", Iran, Mar. Pet. Geol., **21**, 829-843.

39. Sepehr, M. and Cosgrove, J.W. (2005). "Role of the Kazerun Fault Zone in the Formation and Deformation of the Zagros Fold-Thrust Belt, Iran", *Tectonics*, **24**(TC5005), doi:10.1029/2004TC001725.

40. Sherkati, S. and Letouzey, J. (2004). "Variation of Structural Style and Basin Evolution in the Central Zagros (Izeh Zone and Dezful Embayment), Iran", Mar. Petr. Geol., **21**, 535-554.

41. Stocklin, J. (1968). "Structural History and Tectonics of Iran; A Review", American Association of Petroleum Geologist Bulletin, **52**(7), 1229-1258.

42. Stocklin, J. (1974). "Possible Ancient Continental Margins in Iran", In C.A. Burk and C.L. Drake (Eds.), *The Geology of Continental Margins*, 873-887, New York, Springer.

43. Stoneley, R. (1981). "The Geology of the Kuh-e Dalneshin Area of Southern Iran, and Its Bearing on the Evolution Southern Tethys", *J. R. Soc. London*, **138**, 509-526.

44. Takin, M. (1972). "Iranian Geology and Continental Drift in the Middle East", *Nature*, **235**, 147-150.

45. Talebian, M. and Jackson, J. (2004). "A Reappraisal of Earthquake Focal Mechanisms and Active Shortening in the Zagros Mountains of Iran", *Geophys. J. Int.*, **156**, 506-526.

46. Tatar, M., Haztfeld, D., Martinod, J., Walpersdorf, A., Ghafory-Ashtiany, M., and Chéry, J. (2002). "The Present-Day Deformation of the Central Zagros from GPS Measurements", Geophys. Res. Lett., **29**, 1927, doi:10. 1029/2002GL015427.

47. Tchalenko, J.S. and Braud, J. (1974). "Seismicity and Structure of Zagros (Iran): The Main Recent Fault between 33_ N and 35_N", Philos. Trans. R. Soc. London, **277**, 1-25.

48. Vernant, P., et al (2004). "Contemporary Crustal Deformation and Plate Kinematics in Middle East Constrained by GPS Measurements in Iran and Northern Oman", *Geophys. J. Int.*, **157**, 381-398.

49. Walpersdorf, A., Hatzfeld, D., Nankali, F., Tavakoli, F., Nilforoushan, F., Tatar, M., Vernant, P., Chéry, J., and Masson, F. (2006). "Difference in the GPS Deformation Pattern of North and Central Zagros (Iran)", *Geophysical Journal International*, in press.

50. Wells, D.L. and Coppersmith, K.J. (1994). "New Empirical Relationships Among Magnitude, Rupture Length, Rupture Width, Rupture Area and Surface Displacement", Bull. Seism. Soc. Am., **84**, 974-1002.

51. Yamini-Fard, F., Hatzfeld, D., Tatar, M., and Mokhtari, M. (2006). "Microseismicity on the Kazerun Fault System (Iran): Evidence of a Strike-Slip Shear Zone and a Thick Crust", *Geophys. J. Int.*, in press.